J. Membrane Biol. 151, 189–200 (1996)

The Journal of
Membrane
Biology

Activation of Cl^- Currents in Cultured Rat Retinal Pigment Epithelial Cells by Intracellular Applications of Inositol-1,4,5-triphosphate: Differences Between Rats with Retinal Dystrophy (RCS) and Normal Rats

O. Strauss[1], **M. Wiederholt**[1], **M. Wienrich**[2]

[1]CNS Pharmakology, Boehringer Ingelheim, Binger Strasse, 55216 Ingelheim am Rhein, Germany
[2]Institut für Klinische Physiologie, Klinikum Benjamin-Franklin der Freien Universität Berlin, Hindenburgdamm 30, 10122 Berlin

Received: 17 July 1995/Revised: 31 January 1996

Abstract. Using the whole-cell configuration of the patch-clamp technique, we studied the conditions necessary for the activation of Cl^--currents in retinal pigment epithelial (RPE) cells from rats with retinal dystrophy (RCS) and nondystrophic control rats. In RPE cells from both rat strains, intracellular application of 10 μM inositol-1,4,5-triphosphate (IP3) via the patch pipette led to a sustained activation of voltage-dependent Cl^- currents, blockable by 1 mM 4,4′-diisothiocyanatostilbene-2,2′-disulfonic acid (DIDS). IP3 activated Cl^- currents in the presence of a high concentration of the calcium chelator BAPTA (10 mM) in the pipette solution, but failed to do so when extracellular calcium was removed. Intracellular application of 10^{-5}M Ca^{2+} via the patch pipette also led to a transient activation of Cl^- currents. When the cells were preincubated in a bath solution containing thapsigargin (1 μM) for 5 min before breaking into the whole-cell configuration, IP3 failed to activate voltage-dependent currents. Thus, IP3 led to release of Ca^{2+} from cytosolic calcium stores. This in turn activated an influx of extracellular calcium into the submembranal space by a mechanism as yet unknown, leading to an activation of calcium-dependent chloride currents. In RPE cells from RCS rats, which show an increased membrane conductance for calcium compared to normal rats, we observed an accelerated speed of Cl^--current activation induced by IP3 which could be reduced by nifedipine (1 μM). Thus, the increased membrane conductance to calcium in RPE cells from RCS rats changes the response of the cell to the second messenger IP3.

Key words: RPE — Inositol-1,4,5-triphosphate — Cl^- currents — RCS rat — Retinal degeneration

Correspondence to: O. Strauss

Introduction

The retinal pigment epithelium (RPE) is a monolayer of cells located between the neuronal retina and the choriocapillaris. The RPE interacts closely with the retina and is important for maintaining retinal function (Steinberg, 1985). As part of the retina/blood barrier it transports ions and nutrients between the retina and choriocapillaris. The RPE takes part in the daily regeneration of photoreceptors by phagocytosis of shed membranes from photoreceptor outer segments. In addition, it compensates for the changes of subretinal ion concentration induced by light. Since electrical properties of the cell membrane are involved in these functions of RPE, considerable attention has been directed to the underlying ion conductances. Using the whole-cell configuration of the patch-clamp technique in freshly isolated or cultured RPE cells, sodium, potassium, calcium and chloride channels have been described (Hughes & Steinberg, 1990; Ueda & Steinberg, 1992; Botchkin & Matthews, 1993, 1994; Hughes & Segawa, 1993; Strauss et al., 1993; Strauss & Wienrich, 1993, 1994; Tao, Rafuse & Kelly, 1994; Wen et al., 1993, 1994; Ueda & Steinberg, 1994). Investigation of the RPE contribution to the electroretinogram aroused increasing interest in chloride conductances (Gallemore & Steinberg, 1989*a,b;* Griff, 1991; Fujii et al., 1992; LaCour, 1992; Bialek & Miller, 1994). The chloride conductance of RPE has been shown to be activated by cAMP in amphibian RPE cells (Hughes & Segawa, 1993). In addition, Ueda and Steinberg (1994) and Botchkin and Matthews (1993) observed chloride currents induced by hypo-osmotic swelling in rat RPE cells. Whereas Botchkin and Matthews (1993) concluded that the mechanism for activation of chloride currents remained unknown, Ueda and Steinberg (1994) were able to show that intracellular calcium is necessary for activation.

The RCS rat is an animal model for an inherited retinal degeneration which is caused by a malfunction of the RPE. It has been shown that the RPE in this animal is unable to phagocytose shed photoreceptor outer segments (McLaren et al., 1982; Chaitin & Hall, 1983; Hall & Abrams, 1991). This defect has also been demonstrated in cultured RPE cells from RCS rats (Chaitin & Hall, 1983; Hall & Abrams, 1991). Phagocytosis by RPE cells is regulated by the Ca^{2+}/inositol-second messenger pathway (Hall, Abrams & Mittag, 1991; Rodriguez de Turco, Gordon & Bazan, 1992; Heth & Marescalchi, 1994). Several lines of evidence point to a disturbed second messenger system incorrectly regulating the phagocytosis in RCS RPE cells (Gregory, Abrams & Hall, 1992; Heth & Schmidt, 1992; McLaren et al., 1992; Heth & Marescalchi, 1994). An increased membrane conductance for Ca^{2+} compared to normal rats has been shown in cultured RPE cells from RCS rats and possibly contributes to this incorrect regulation (Strauss & Wienrich, 1993).

We used the whole-cell configuration of the patch-clamp technique (Hamill et al., 1981) to look for second-messenger mechanisms which activate Cl^- currents in RPE cells and to compare the reaction of the second-messenger systems in cells from RCS and nondystrophic rats. For this purpose, inositol-1,4,5-triphosphate was intracellularly applied via the patch pipette to RPE cells. We found that IP3 induced a chloride conductance. The speed of chloride current activation was increased in RPE cells from RCS rats compared to nondystrophic rats.

Materials and Methods

Cell Culture

Primary cultures of rat retinal pigment epithelial cells were established using the method of Edwards (1977). The eyes of pigmented (hooded) rats were stored overnight in Puck's saline F (Puck, Cieciura & Robinson, 1958) at room temperature. After incubation in trypsin for 35 min at 37°C (0.1% trypsin in Puck's saline F without Ca^{2+} and Mg^{2+}), the eyes were opened by a circumferential incision just posterior to the ora serrata and the anterior parts of the eye and neural retina were removed revealing the apical surface of the RPE. Sheets of the RPE were gently brushed off the choroid and collected in Ham's F10 culture medium supplemented with 20% fetal calf serum, 100 μg/ml kanamycin and 50 μg/ml gentamycin. After the sheets were partially dissociated by gentle pipetting, the cell suspension was plated out into petri dishes equipped with glass coverslips. The cultures were maintained at 37°C and 5% CO_2 in air. The medium was changed twice a week. After 24 hr, the RPE cells had settled down and started to spread out. The cultures resulted in confluent monolayers of pigmented and polygonal shaped cells after 9–20 days.

Patch-Clamp Recordings

Patch-clamp recordings were performed at room temperature. Coverslips with subconfluent primary cultures (3–9 days in culture) were placed into a perfusion chamber which was mounted on the stage of an inverted microscope. During the patch-clamp recordings, the cells were superfused with the solutions indicated in the Table. The bath solutions were iso-osmotic to Ham's F10 culture medium. Patch electrodes of 3–5 MΩ resistance were pulled from borosilicate glass tubing (Hilgenberg, Malsfeld, Germany) using a Zeitz DMZ electrode puller (Zeitz, Augsburg, Germany). The patch pipettes were filled with the pipette solutions containing (mM): (1) standard pipette solution: 100 Cs-methanesulfonate, 20 NaCl, 2 $MgCl_2$, 10 HEPES, 5.5 EGTA, 0.5 $CaCl_2$ (2) BAPTA-pipette solution: 100 Cs-methanesulfonate, 20 NaCl, 2 $MgCl_2$, 10 BAPTA, 10 HEPES (3) 10^{-5} M-Ca^{2+}-pipette solution: 110 Cs-methanesulfonate, 20 NaCl, 2 $MgCl_2$, 10 HEPES, 0.01 $CaCl_2$. All solutions were adjusted to pH = 7.2 with Tris. When using EGTA together with calcium the concentration of the free calcium was calculated using a dissociation constant of 0.15 μM (Neher, 1988). IP3 was freshly added from stock solutions to the final concentrations of 10 μM. To avoid activation of swelling-induced currents the pipette solution was hypo-osmotic to the bath solution (app. 60 mOsm; estimated using the Vapor Pressure Osmometer 5100 B; Wescor, Logan, Utah). Whole-cell currents were measured with an EPC-7 patch-clamp amplifier (List Medicals, Darmstadt, Germany) and filtered at 3 kHz lowpass. Electrical stimulation, data storage and analysis were performed using the TIDA hard- and software (Battelle, Frankfurt, Germany) in conjunction with an AT-compatible computer. The reference electrode was connected to the bath solution by a liquid junction consisting of a plastic tube filled with control ringer to minimize changes in the liquid junction potential when the bath solution was changed. Changing the bath solution from control ringer to low-chloride ringer led to a change of the electrode offset potential of −3 mV in 30 min and to a change of the liquid junction potential of +10.7 mV. The liquid junction potential was estimated according to the method described by Neher (1992). All stated potential values were corrected for the liquid junction potential. After establishing the whole-cell configuration, the membrane capacitance and the access-resistance were compensated within 10–45 sec. The values of membrane capacitance and access-resistance were estimated 10–15 min after establishing the whole-cell configuration. The access resistance was determined by a single-exponential fit of the relaxation of the transient capacitative current, which was induced by a 10-mV voltage step for 30 msec from the holding potential to depolarize the cell. The exponential fit revealed the time constant of the membrane capacitance. The ratio of the time constant to the membrane capacitance yielded the access resistance.

Table. Composition of the bath solutions

	Control Ringer	Low-Cl^- Ringer	High-Ca^{2+} Ringer	Ca^{2+}-free Ringer
NaCl	135		120	137
Na-methanesulfonate		120		
$CaCl_2$	1	5	10	
Ca-gluconate		5		
$MgCl_2$	0.6	0.6	0.6	0.6
HEPES	33	33	33	33
TEACl	10	10	10	10
EGTA				1
Glucose	6.1	6.1	6.1	6.1

The pH was adjusted to 7.2 with Tris. The concentrations of the components are given in mM. EGTA = ethylene glycol bis(2-aminoethylether)-N,N,N′,N-tetraacetic acid, HEPES = N-(2- Hydroxyethyl)piperazine-N′-2-ethane sulfonic acid, TEAC1 = tetraethylammonium chloride.

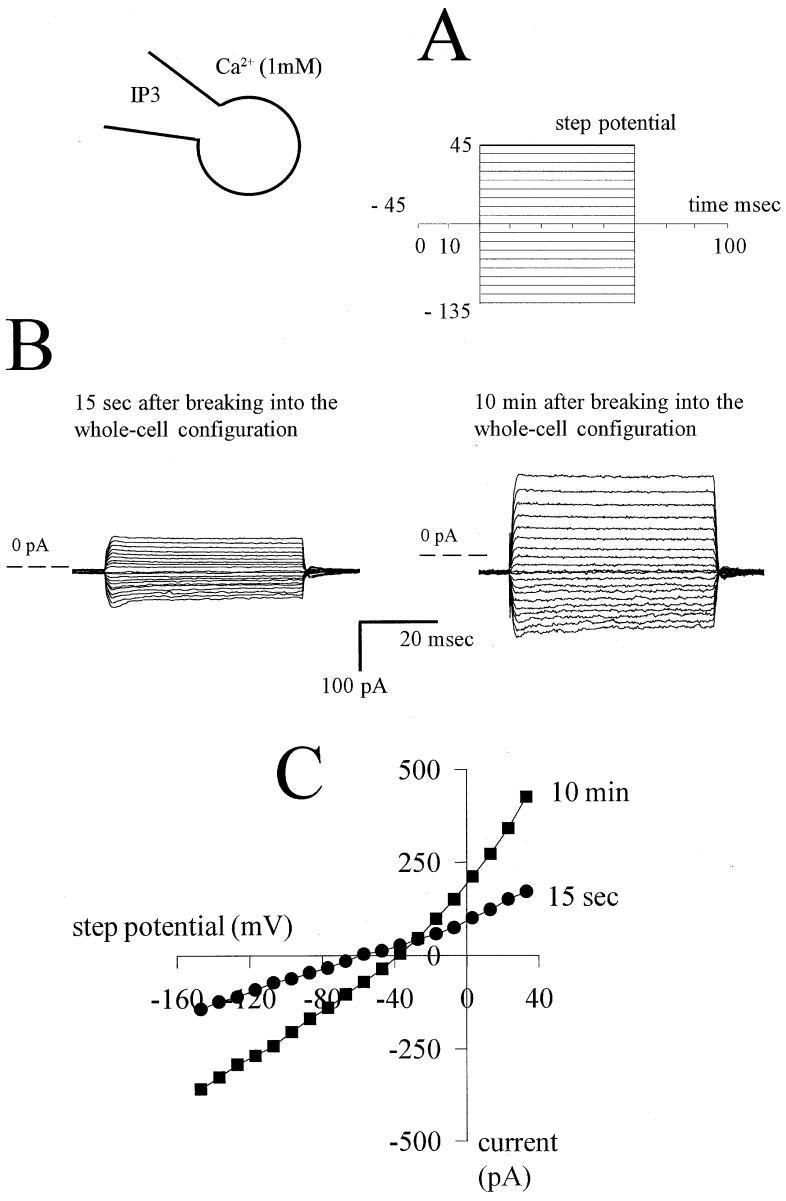

Fig. 1. Induction of voltage-dependent currents by intracellular application of IP3. (*A*) Pattern of electrical stimulation: The cell was depolarized from the holding potential (HP = −45 mV) by nine voltage steps of 10 mV increasing amplitude and 50 msec duration and then hyperpolarized by nine voltage steps of 10 mV increasing amplitude 50 msec duration. (*B*) Left panel: Currents (induced by the electrical stimulation shown in Fig. 1*A*) 15 sec after establishing the whole-cell configuration with control ringer (*see* Table) as bath solution and standard-pipette solution with 10 μM IP3 in the pipette. Right panel: Currents induced in the same cell 10 min after breaking into the whole-cell configuration (cell capacitance 27 pF). (*C*) Current/voltage plot of the experiment shown in Fig. 1*B:* Amplitudes of the steady state currents were plotted against the potentials (corrected for liquid junction potential) of the voltage-steps of the stimulation protocol (Fig. 1*A*). After 15 sec in the whole-cell configuration (circles), no voltage-dependent currents were observed; 10 min later voltage-dependent currents could be observed (squares).

The membrane capacitance was estimated by integration of the area below the transient capacitance current curve of the same voltage step. The membrane capacitance was 7–40 pF (n = 101) or 23.4 ± 5 pF (SEM; n = 10) and the access resistance was 10–18 MΩ (n = 101) or 14.4 ± 1 MΩ (SEM; n = 10).

The figures show one typical experiment out of 3–6 performed. Data are presented as mean ± SEM. Statistical analysis was performed using Student's unpaired t-test. Significance was considered at P-values lower than 0.05.

Media and supplements for cell culture were purchased from Gibco Life-Technologies (Eggenstein, Germany). The chemicals were from Sigma (Deisenhofen, Germany), Serva (Heidelberg, Germany), Calbiochem (Bad Soden, Germany) and E. Merck (Darmstadt, Germany).

Results

Intracellularly Applied IP3-induced Voltage-dependent Currents

We used the whole-cell configuration for intracellular application of IP3 via the patch pipette to cultured RPE cells. In the first set of experiments, intra- and extracellular calcium concentrations were held at physiological levels. We used extra- and intracellular potassium-free conditions to eliminate superimposed potassium currents. The cells were superfused by the control ringer

(Table) and the patch pipette contained the standard pipette solution to establish intra- and extracellular physiological calcium concentrations. Directly after breaking into the whole-cell configuration, the cells showed a resting potential of −53.2 ± 9 mV ($n = 15$). At this point, the cells had not yet been dialyzed by the pipette solution and residual potassium currents were present. The cells were clamped to −45 mV. Under these conditions, the cells were electrically stimulated directly after establishing the whole-cell configuration with 10 μM IP3 in the pipette solution using a series of voltage-steps positive and negative from the holding potential (Fig. 1*A*). Immediately after breaking into the whole-cell configuration, no voltage-dependent currents could be observed (Fig. 1*B*). After a time delay of 20–200 sec, the cell started to depolarize, and membrane conductance started to increase. 7–10 min later, the electrical stimulation led to maximal voltage-dependent currents (Fig. 1*B* and *C*) and the cells showed a resting potential of −23 ± 1.9 mV ($n = 4$). Thus, IP3 activated voltage-dependent currents.

The Currents Induced by IP3 were Mainly Carried by Cl^--Ions

To characterize the IP3-induced currents, the extracellular Cl^--concentration was varied after the currents had reached maximal amplitudes (after 7–10 min). In a first set of experiments, the IP3 currents were stimulated by depolarization (Fig. 2*A*). These currents (Fig. 2*B*) were reversibly reduced to 59.5 ± 4.4% ($n = 3$) of control when the chloride concentration in the bath was reduced from 151.2 mM to 21.2 mM (recovery occurred to 105 ± 7%; $n = 3$, *not shown*). Thus, IP3-induced currents were decreased when the chemical gradient for chloride was reduced.

In a second set of experiments, we studied the shift of the reversal potential (zero current potential) of the IP3-induced currents (Fig. 2*C*). The reversal potential was estimated from current/voltage plots where maximal current amplitudes were plotted against the step potentials (Fig. 2*C*) of the electrical stimulation (shown in Fig. 1*A*, from a holding potential of 0 mV). Using the high-calcium ringer (Table) as bath solution, a reversal potential of $E_{rev} = -33.8 \pm 1.2$ mV ($n = 4$) was observed. Changing the bath solution to the low-chloride ringer resulted in a reversal potential of +0.4 ± 1.5 mV ($n = 4$). The calculated Nernst' potentials for Cl^- were $E_{Cl} = -45$ mV with high-calcium ringer (high extracellular chloride concentration) and $E_{Cl} = +2$ mV with low-chloride ringer. Addition of the chloride channel blocker 4,4′-diisothiocyanatostilbene-2,2′-disulfonic acid (DIDS, 1 mM) to the bath solution led to a reversal block of the outward currents to 7.8 ± 6% ($n = 4$) of control (recovery occurred to 63 ± 11%; $n = 4$). The chloride conductance showed nonlinear voltage-dependence under strictly symmetrical chloride concentrations, excluding that rectification resulted from different chloride concentrations. Thus, the IP3-induced currents were mainly carried by chloride ions and expressed characteristics of an outward rectifier.

IP3-induced Currents were Calcium-dependent Chloride Currents

To characterize more closely the mechanism by which IP3 activated the chloride currents, we used a pipette solution containing 10 mM BAPTA, a calcium chelator, to adjust the cytosolic calcium concentration to zero. For maximal stimulation of calcium-dependent mechanisms, we used 10 mM calcium in the bath solution (high-calcium ringer, Table). The holding potential was 0 mV to eliminate overlying calcium conductances (McDonald et al., 1994). With 10 μM IP3 in the pipette, an outwardly directed membrane conductance was activated (Fig. 3*B*, inlay; Fig. 3*C* bottom) comparable to the conductance shown in Fig. 1. The currents activated and deactivated nearly time-independent and showed inactivation at very positive step potentials. Under these conditions, a maximal stimulation of chloride currents with 113.4 ± 13 $pApF^{-1}$ was observed. Thus, an increase of cytosolic-free calcium seems not to be necessary for activation of chloride currents by IP3. In the next step, the effects of IP3 under extra- and intracellular calcium-free conditions were studied. The cells were superfused with calcium-free bath solution (Table 1). The patch pipette contained 10 μM IP3 in the BAPTA-pipette solution. Under these conditions, IP3 failed to induced voltage-dependent currents (Fig. 4). Thus, IP3 activates calcium-dependent chloride currents by stimulating an influx of extracellular calcium into the cell.

To provide further evidence for calcium-dependent chloride currents, the effect of directly increasing the cytosolic calcium concentration was investigated. For this purpose, calcium was intracellularly applied via the patch pipette (Fig. 5). In these experiments, the cells were superfused by control ringer (Table) and the patch pipette contained the 10^{-5} M-calcium-pipette solution. Breaking into the whole-cell configuration under these conditions resulted in a transient increase of the membrane conductance. A current/voltage plot at the moment of maximal current amplitudes (Fig. 5*B*) showed that intracellularly applied calcium led to currents comparable to those induced by IP3 (*see* Fig. 3). The reversal potential of the calcium-induced currents was −43.1 ± 2 mV ($n = 4$). With 10^{-4} M calcium in the patch pipette no activation of voltage-dependent currents was observed (*not shown*). Thus, intracellularly applied calcium transiently activated chloride currents.

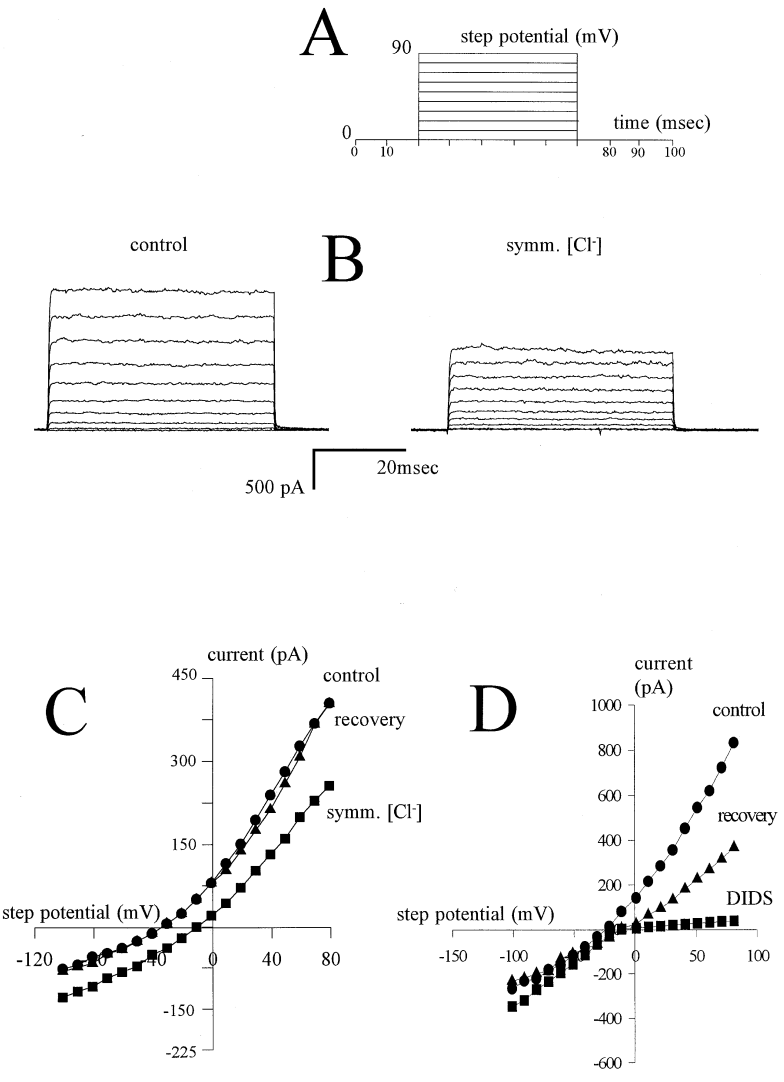

Fig. 2. Identification of currents induced by IP3. (*A*) Pattern of electrical stimulation. The cell was depolarized using 9 voltage steps with 10 mV increasing amplitude and 50 msec duration in 1-sec intervals (HP = 0 mV). (*B*) Left: Currents induced by depolarization (*see* Fig. 2*A*) when the IP3-induced currents reached maximal amplitudes under control conditions (high-calcium ringer as bath solution (Table), standard pipette solution). Under these conditions a chemical gradient for chloride directed into the cell is present. Right: Reduced currents induced by depolarization of the same cell after changing the bath solution to low-chloride ringer (Table) so that symmetrical chloride concentrations exist on both sides of the membrane (cell capacitance 19 pF). (*C*) In a second set of experiments, the reversal potentials of the IP3-induced currents were investigated. This experiment is depicted as a current/voltage plot (potentials corrected for liquid junction potential). The cell was electrically stimulated using the stimulation protocol shown in Fig. 1*A* (HP = 0 mV) and the steady-state currents were plotted against their step potentials. Under extra- and intracellular asymmetrical chloride concentrations (standard pipette solution, the high-calcium ringer shown in Table) the maximal IP3-induced currents showed a reversal potential of −37.7 mV (triangles). With symmetrical chloride concentrations on both sides of the membrane (standard pipette solution, the low chloride ringer in Table), the currents showed a reversal potential of 0 mV (squares) which was reversible when the bath solution was switched back to high-calcium ringer (circles). The cell capacitance was 41 pF. (*D*) Effect of the Cl^--channel blocker DIDS: The experiment is depicted as current/voltage plot (potentials corrected for liquid junction potential). The maximal current amplitudes were plotted against their step potentials of the electrical stimulation protocol (shown in Fig. 1*A;* holding potential HP = 0 mV). Extracellular application of 1 mM DIDS (squares) led to a reversible (triangles) block of the voltage-dependent outward current (circles).

Involvement of Cytosolic Calcium Stores

As shown in Fig. 4, IP3 induced chloride currents only when extracellular calcium was present. To test if IP3 directly increased the calcium permeability of the cell membrane, or if IP3 led to the release of calcium from IP3-sensitive calcium stores which in turn lead to an influx of extracellular calcium into the cell, the effects of high intracellular BAPTA concentrations (Fig. 6) and of thapsigargin (Fig. 7) were studied. High intracellular concentrations of BAPTA are known to passively deplete intracellular calcium stores (Hoth & Penner, 1993). Therefore, the whole-cell configuration was established with 10 mM calcium in the bath and 10 mM BAPTA in the pipette solution without IP3. The cells depolarized to a resting potential of −21.1 ± 1 mV (n = 5). After 7–10 min, the cells showed voltage-dependent currents with maximal current amplitudes of 2.2 ± 0.4 $pApF^{-1}$ (n = 5). The currents induced by BAPTA were comparable to those induced by IP3 (Fig. 6*A* and *B*). However, the maximal current amplitudes induced by BAPTA were much smaller (112 ± 15 pA; n = 5) than those induced by IP3 (2833 ± 488 pA; n = 5).

Thapsigargin is known to inhibit the ATPases of calcium stores and to release calcium from cytosolic calcium stores without the formation of IP3. The cells were preincubated for 5 min with 1 μM thapsigargin in standard bath solution (Table) before establishing the whole-cell configuration with 10 mM BAPTA and 10μM IP3 in the pipette solution. Under these conditions, IP3 failed

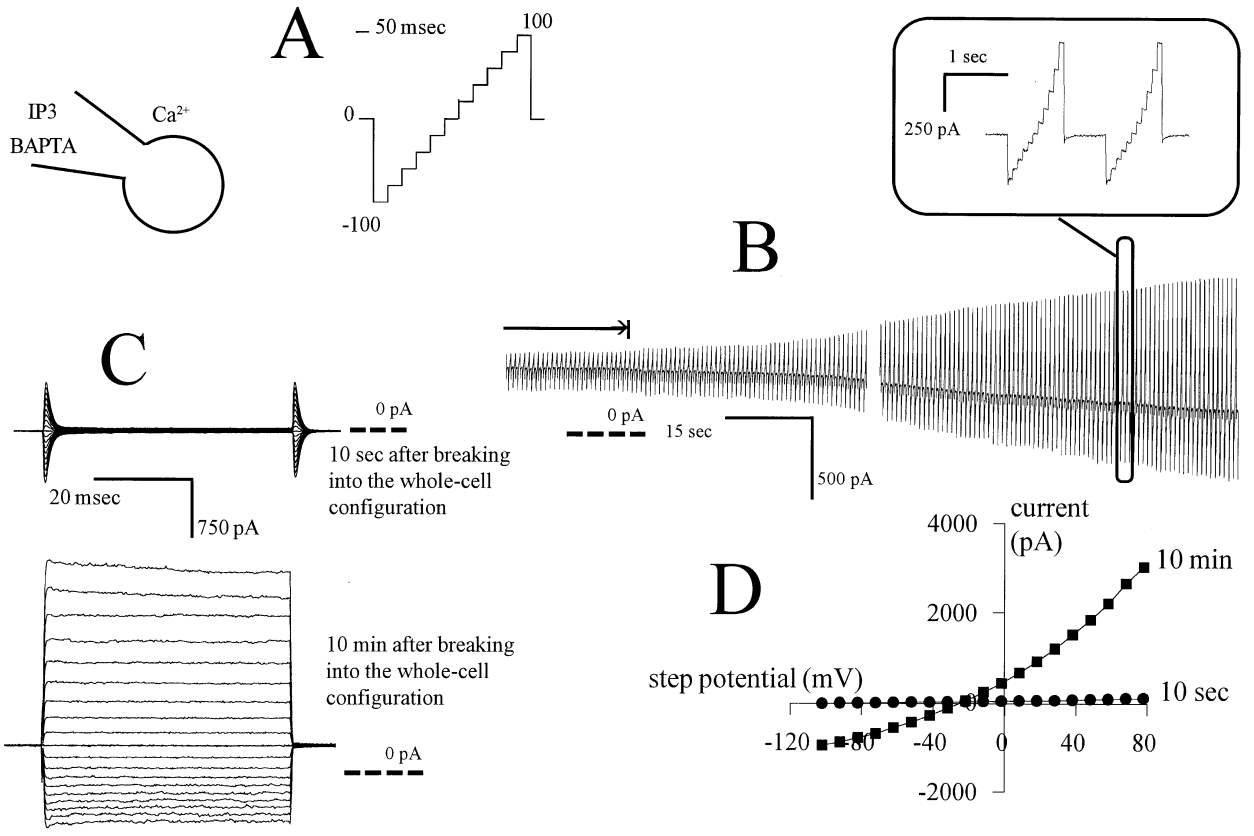

Fig. 3. Maximal stimulation of Cl^- currents by IP3 with 10 mM Ca^{2+} in the bath and 10 mM BAPTA in the pipette. (*A*) For continuous recording of the membrane conductance, the cell was electrically stimulated every 0.5 sec. From the holding potential of 0 mV, the cell was hyperpolarized to −100 mV and then depolarized stepwise to +100 mV (step duration was 50 msec, step increment was +20 mV). (*B*) Continuous recording of the membrane conductance when IP3 was applied intracellularly to the cell. The cell was stimulated using the stimulation protocol shown in Fig. 3*A*. The recording started 15 sec after breaking into the whole-cell configuration with the patch pipette containing BAPTA-pipette solution with IP3 (10 μM). After a time delay of 25 sec (indicated by the arrow) the membrane conductance started to increase showing increasing amplitudes with increasing depolarization (inlay). The cell capacitance was 29 pF. (*C*) Time-dependent behavior of the IP3-induced currents. The cell was electrically stimulated using the stimulation protocol shown in Fig. 1*A* with a holding potential of 0 mV. Left: Ten seconds after breaking into the whole-cell configuration, the electrical stimulation led to residual capacitance artifacts and no voltage-dependent currents were observed. Right: Ten minutes after breaking into the whole-cell configuration, the electrical stimulation led to voltage-dependent currents which activated nearly time-independently and showed a weak inactivation at very positive step potentials (cell capacitance 36 pF). (*D*) Current/voltage plot of the steady state currents shown in *C*. The steady-state current amplitudes were plotted against the potentials (corrected for liquid-junction potential) of the voltage-steps of the stimulation protocol. Ten seconds after breaking into the whole-cell configuration with 10 μM IP3 in the patch pipette (circles), the nearly linear current/voltage relationship of the membrane conductance indicated the absence of voltage-dependent currents. Ten minutes after breaking into the whole-cell configuration (squares), the cell showed increasing current amplitudes induced by de- or hyperpolarization.

to induce voltage-dependent currents (Fig. 7). Thus, depletion of calcium stores by thapsigargin preincubation prevented the effect of IP3 in cultured rat RPE cells. Therefore it seems likely that IP3 activates calcium-dependent chloride currents by release of calcium from cytosolic calcium stores which then leads to an influx of calcium into the cell.

Comparison of Cl^--current Activation in Cells from RCS and Nondystrophic Rats

Since the main characteristics of the response to IP3 were identical in RCS and nondystrophic rats, differences in the speed of activation of the current were investigated. In a previous paper, we showed that RPE cells from RCS rats express an increased calcium conductance as compared to cells from nondystrophic rats. This calcium conductance was nifedipine sensitive: 1 μM nifedipine led to a reversible reduction of the maximal current amplitudes to 35 ± 5% ($n = 5$); recovery occurred to 60 ± 5% ($n = 3$). The maximal barium current amplitude of this conductance was in RPE cells control rats 0.75 ± 0.15 $pApF^{-1}$ ($n = 4$) whereas in cells from RCS rats 2.6 ± 0.3 $pApF^{-1}$ ($n = 5$). Our hypothesis was that a faster diffusion of calcium into the cell should result in a faster activation of the chloride conductance. The diffusion rate of calcium is dependent on the con-

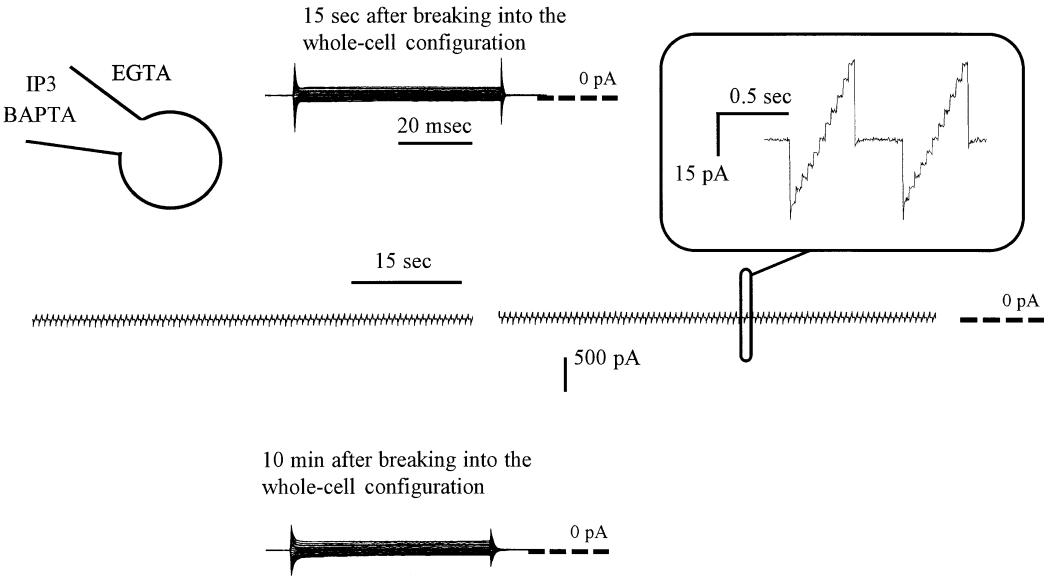

Fig. 4. Effects of intracellularly applied IP3 under extra- and intracellular calcium-free conditions. Effect of IP3 under extracellular calcium-free conditions: The cells were superfused using calcium-free ringer (Table) and the pipette was filled with BAPTA-pipette solution with IP3 (1 μM). Left panel: Currents induced by the electrical stimulation protocol shown in Fig. 1*A* using a holding potential of 0 mV, 15 sec after establishing the whole-cell configuration. Only residual capacitance artifacts were observed but no voltage-dependent currents (cell capacitance 16 pF). Middle panel: Continuous recording of the membrane conductance during the whole-cell configuration with 10 μM IP3 in the pipette solution using the electrical stimulation shown in Fig. 3*A*. The membrane conductance remained unchanged. A magnification of the current deflections (frame) indicates a linear current/voltage relationship and therefore the absence of voltage-dependent currents. Right panel: Currents induced by electrical stimulation shown in Fig. 1*A* from a holding potential of 0 mV, 10 min after breaking into the whole-cell configuration. Under extracellular calcium-free conditions IP3 had no effects on the membrane conductance.

centration gradient for calcium from the extra- to the intracellular space and on the membrane permeability for calcium. Thus, variations of extracellular calcium concentration or a changed membrane permeability for calcium should change the speed of chloride current activation. For this investigation we used the BAPTA-pipette solution with IP3 to control intracellular Ca^{2+} buffer capacity. As bath solution we used control ringer and high-calcium ringer (Table) to test the effects of two different calcium gradients. The activation of chloride currents was monitored using the stimulation protocol shown in Fig. 3*A* from a holding potential of −45 mV. This holding potential keeps L-type calcium channels active. Since the IP3-induced outward currents were almost totally blocked by DIDS (Fig. 2*D*), they were exclusively carried by Cl^- ions. To compare the activation of chloride currents in both cell types, the slope of outward current activation was estimated during the linear phase of current activation (Fig. 8*A*). The slope of current activation was expressed as increase in outward current amplitude within one minute. This was expressed in percent on the control value measured directly after breaking into the whole-cell configuration and is shown in Fig. 8*B*. A faster activation of chloride currents was observed in RPE cells from RCS and nondystrophic rats when a higher concentration gradient for calcium was established using a bath solution with 10 mM calcium (Fig. 8*B*). In addition, in RPE cells from RCS rats, a significantly faster activation of chloride currents than in RPE cells from control rats was observed using both bath solutions. With 1 mM calcium in the bath, the current increase in RPE cells from RCS rats was +190 ± 9% *vs.* +23 ± 7% ($n = 4$) in cells from nondystrophic rats. With 10 mM calcium in the external solution, the current increase in cells from RCS rats was +58 ± 150% *vs.* +155 ± 15% ($n = 5$) in cells from nondystrophic rats. The L-type calcium-channel blocker nifedipine (1 μM) reduced the current increase in RCS RPE cells to +45 ± 16% ($n = 3$) in the presence of 10 mM extracellular calcium which confirms the identity of the Ca^{2+} channel mediating the increased speed of the Cl^- current activation in RPE cells from RCS rats. Thus, the increased membrane conductance for calcium in cells from RCS rats changes the response of the cells to the second messenger IP3.

Discussion

We demonstrated that intracellular application of IP3 to cultured retinal pigment epithelial (RPE) cells from both RCS and nondystrophic rats led to activation of voltage-dependent chloride currents. These chloride currents were calcium-dependent. Cytosolic calcium stores and an influx of extracellular calcium into the cell were in-

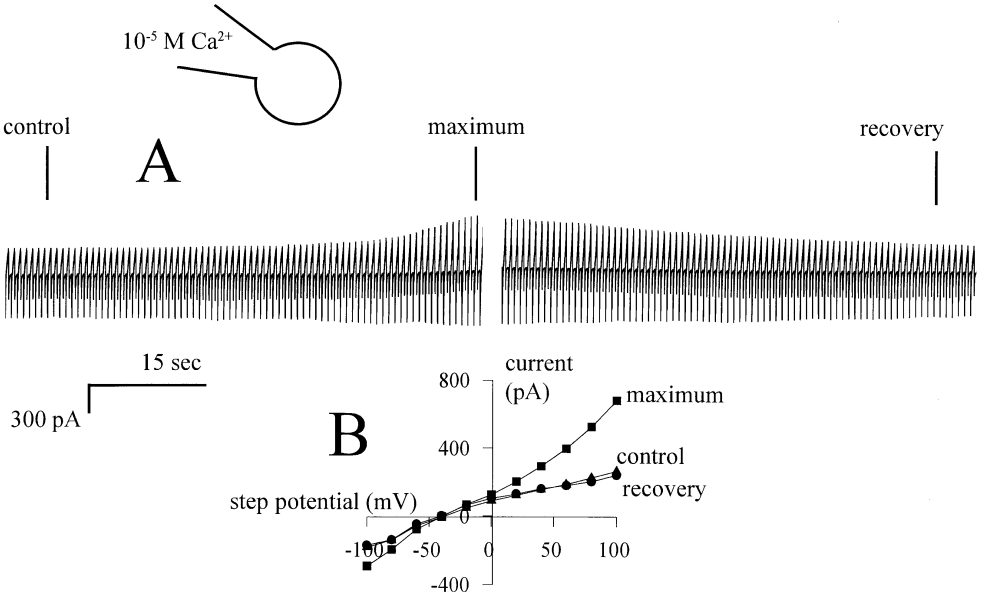

Fig. 5. Activation of Cl^- currents by intracellular application of Ca^{2+}. (*A*) Continuous recording of the membrane conductance using the stimulation protocol shown in Fig. 3*A*. The stimulation started 10 sec after breaking into the whole-cell configuration with the 10^{-5} M-Ca^{2+}-pipette solution. After 40 sec the current deflections induced by the electrical stimulation increased transiently and decreased to the control level (cell capacitance 16 pF). (*B*) Current/voltage plot of the currents at the times indicated in *A*. Steady state currents were plotted against the step potentials (corrected for liquid junction potential) of the electrical stimulation shown in Fig. 3*A*. The conductance in the control period (triangles) showed a linear current/voltage relationship indicating the absence of voltage-dependent currents. When the Ca^{2+}-effect was maximal (squares), the cell showed voltage-dependent currents with a reversal potential of -42.9 ± 2 mV ($n = 4$). After 50 sec the membrane conductance recovered to the control level (circles). Thus, intracellular application of Ca^{2+} led to a transient activation of Cl^--currents.

volved in the activation of these currents. The L-type calcium conductance which provides the increased membrane conductance for calcium in RPE cells from RCS rats led to an accelerated activation of the IP3-induced chloride conductance in these cells.

The IP3-induced Conductance

Intracellular application of IP3 via the patch-pipette led to an activation of voltage-dependent currents. Since establishing extra- and intracellularly symmetrical chloride concentrations shifted the reversal potential to zero and the currents could be blocked by DIDS, the IP3-induced currents could be identified as chloride currents. The voltage-dependent outward currents were more affected by DIDS than the inward currents. This has also been reported by other groups investigating chloride currents in RPE cells (Botchkin & Matthews, 1993; Ueda & Steinberg, 1994). Under asymmetrical concentrations for chloride, the reversal potential of the IP3-induced currents did not correspond exactly to the Nernst potential for chloride. A possible explanation for this observation is that many chloride channels show a certain permeability for methanesulfonate-ions, the chloride substitute used in these experiments. Chloride or anion conductances in T84 colonic cells (Halm & Frizzell, 1992), lymphocytes (Calahan & Lewis, 1988) and P-glycoprotein expressing MDR1 cells (Valverde et al., 1992) have been shown to conduct gluconate or methanesulfonates. A similar suggestion was made by Botchkin and Matthews (1993) for swelling-induced chloride currents in cultured rat RPE cells.

Since IP3 failed to activate chloride currents under intra- and extracellular calcium free conditions, and since the effect of IP3 could be mimicked by intracellular application of calcium, IP3 induced a calcium-dependent chloride conductance. Ueda and Steinberg (1994) could also demonstrate the activation of chloride currents by directly increasing the cytosolic calcium concentration using a calcium ionophore in pretreated cells in calcium-free bath solution. Like Ueda and Steinberg (1994) and Botchkin and Matthews (1993), we failed to activate chloride currents using a ionophore in combination with calcium in cells which were not pretreated (*data not shown*). The reason for this remains unknown.

In addition, we showed that IP3 induces an influx of extracellular calcium into the cell which in turn activates calcium-dependent chloride currents. This hypothesis was supported by the observation that the reversal potential of IP3-induced currents was significantly more positive than that of currents activated by intracellularly applied calcium. IP3 must increase the calcium permeability of the cell membrane to induce an influx of extracellular calcium into the cell for activation of calcium-dependent chloride currents. The additional calcium per-

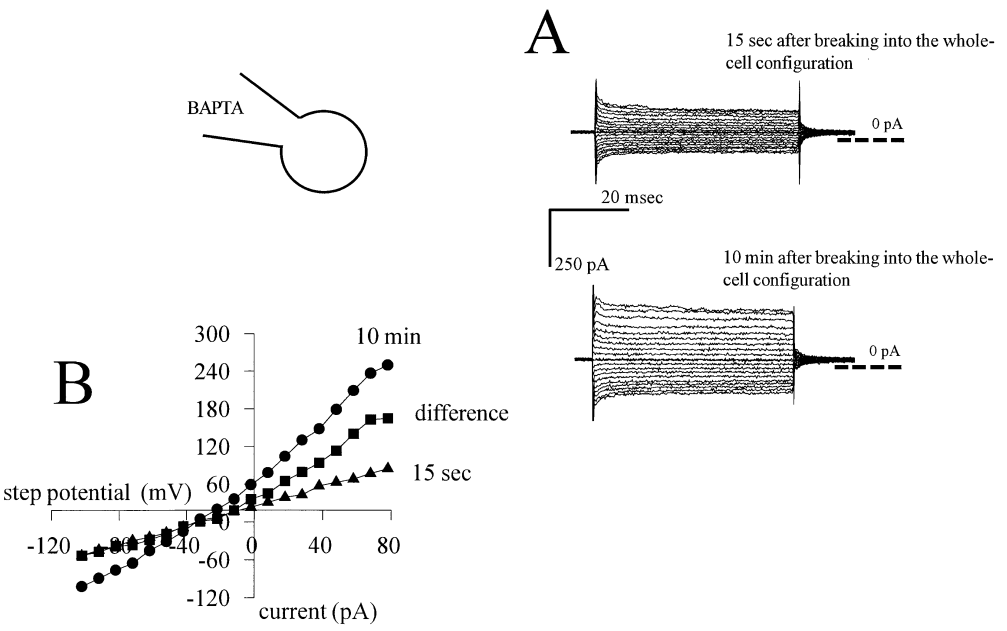

Fig. 6. BAPTA-induced voltage-dependent currents. (*A*) Effect of intracellularly applied BAPTA (10 mM) on the membrane conductance. Top: Currents induced 15 sec after breaking into the whole-cell configuration using the electrical stimulation protocol shown in Fig. 1*A*. The pipette contained BAPTA-pipette solution. No voltage-dependent currents were observed. Bottom: After 10 min in the whole-cell configuration, the same electrical stimulation induced voltage-dependent currents (cell capacitance 29 pF). (*B*) Current/voltage plot of the experiment shown in *B*. The steady-state current amplitudes were plotted against the potentials (corrected for liquid junction potential) of the voltage steps of the electrical stimulation. Fifteen seconds after breaking into the whole-cell configuration (triangles), the cell showed a passive membrane conductance with voltage-independent currents. Ten minutes after breaking into the whole-cell configuration (circles), the electrical stimulation led to increasing voltage-dependent currents in response to increasing depolarization of the cell. Calculating the difference between the currents measured directly after breaking into the whole-cell configuration and the currents measured 10 min after breaking into the whole-cell configuration yielded the BAPTA-induced currents (squares).

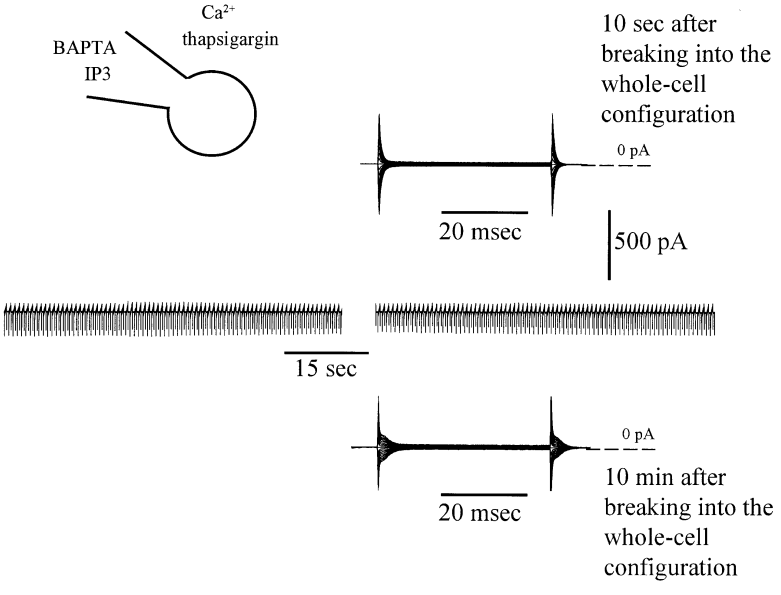

Fig. 7. Effect of IP3 on cells preincubated in thapsigargin. Before breaking into the whole-cell configuration the cell was preincubated in 1 μM thapsigargin for 5 min. Upper trace: Directly after breaking into the whole-cell configuration with the BAPTA-pipette solution with IP3 (10 μM), the cell (cell capacitance 12 pF) was electrically stimulated using the stimulation protocol shown in Fig. 1*A* (HP = 0 mV). The electrical stimulation led only to residual capacitative artifacts. Middle trace: In a continuous recording of the membrane conductance no changes of the currents induced by the electrical stimulation shown in Fig. 3*A* were observed. Lower trace: After 10 min in the whole-cell configuration no voltage-dependent currents could be detected (stimulation protocol in Fig. 1*A*, HP = 0 mV). Thus, in cells preincubated with thapsigargin, intracellularly applied IP3 failed to activate chloride currents.

meability shifts the reversal potential of the IP3-induced currents to more positive values. The influx of extracellular calcium into the cell may occur via direct opening of calcium channels by IP3 (Kuno & Gardner, 1987; Kuno et al., 1994) or by increasing the membrane conductance for calcium by release of calcium from cytosolic IP3-sensitive calcium stores (Marty & Tan, 1989; Matthews, Neher & Penner, 1989; Hoth & Penner, 1993;

Kirischuk et al., 1995). In our investigation, IP3 failed to activate currents when the cells were preincubated with thapsigargin. As has been observed by Kirischuk et al. (1995), thapsigargin showed no acute effect in our experiments but needed 5 min of incubation to prevent the effect of IP3. In addition, BAPTA alone activated chloride currents, however to a much lesser extent than when applied in combination with IP3. This can be explained by the fact that BAPTA (10 mM) is able to passively deplete calcium stores (Hoth & Penner, 1993). Thus, it seems more likely that the calcium influx resulted from depletion of IP3-sensitive calcium stores. This was supported by the fact that in our hands calcium alone only transiently activated the chloride currents, while IP3 led to a sustained activation of currents. Since even in the presence of BAPTA, IP3 was able to activate chloride currents, a simple rise of the cytosolic calcium concentration did not induce an influx of extracellular calcium into the cell. We propose that the action of calcium release from cytosolic stores increases the membrane permeability for calcium. This increase in calcium permeability causes submembranal calcium levels to rise, which in turn activated chloride currents.

The chloride conductance described here was not activated by volume changes. We used a hypo-osmotic pipette solution (difference app. 60 mOsm) to prevent the bath solution from becoming hypo-osmotic to the cytosol during the whole-cell configuration. The cells showed no visible changes in cell volume during the patch-clamp recordings. In addition, the amplitude of the observed chloride currents was clearly dependent upon the nature of the intracellularly applied substances. In the absence of IP3 only a weak activation of chloride conductances was observed. Under extracellular calcium-free conditions no chloride currents were activated in the presence of IP3.

Physiological Role of the IP3-induced Chloride Currents

Chloride conductances have been shown to be of importance for RPE cells. Chloride conductances play a role in volume regulation in RPE cells, an important function when considering that the RPE forms a part of the retina/blood barrier (Botchkin & Matthews, 1993; Ueda & Steinberg, 1994; Kennedy, 1994). In addition, chloride conductances are involved in epithelial chloride transport by the RPE. Chloride conductances activated by cAMP provide an efflux pathway for chloride out of the cell across the basolateral membrane (LaCour, 1992; Fujii et al., 1992; Bialek & Miller, 1994). Finally, chloride conductances are involved in the generation of light-evoked signals from the RPE apparent in the electroretinogram (Gallemore & Steinberg, 1989*a,b;* Joseph & Miller, 1991; Bialek & Miller, 1994).

Here, we describe a calcium-dependent chloride conductance which is activated by depletion of IP3-sensitive calcium stores in rat RPE cells. It has been shown that IP3 is activated in RPE cells in response to several agonists such as neuropeptides (Kuriyama et al., 1992), vasopressin (Friedman et al., 1991), carbachol (Liu et al., 1992) and serotonin (Osborne et al., 1993). IP3 also triggers the onset of phagocytosis (Rodriguez de Turco et al., 1992). In addition, exposing the retina to light increases the IP3 concentration in RPE cells (Rodriguez de Turco et al., 1992) and stimulates a basolateral chloride conductance (Gallemore & Steinberg, 1989*a,b;* Joseph & Miller, 1991). Since we have shown that IP3 also stimulates a chloride conductance in rat RPE cells, we propose that changes of the RPE chloride conductance induced by light are mediated by an increase of the cytosolic IP3 in these cells. IP3 itself may be induced by a substance which diffuses from the retina to the RPE as it has been discussed by Gallemore and Steinberg (1990).

IP3 Response of RPE Cells from RCS Rats

The retinal degeneration in RCS rats is caused by the inability of RPE cells to ingest shed photoreceptor outer segments. The phagocytosis of these membranes is regulated by the IP3/calcium second messenger system. Several investigations point to an impaired regulation of phagocytosis as a consequence of a disturbed second messenger system in the RPE of RCS rats (Gregory, Abrams & Hall, 1992; Heth & Schmidt, 1992; McLaren et al., 1992; Heth & Marescalchi, 1994). In addition, an increased calcium conductance in RPE cells from RCS rats has been reported (Strauss & Wienrich, 1993). Thus, we compared the response to IP3 in RPE cells from RCS and nondystrophic rats. We studied the activation of chloride currents in both species which was dependent on an influx of extracellular calcium into the cell. We could show that the activation of chloride currents was dependent on the diffusion rate of calcium into the cell. With a higher gradient for calcium into the cell, we observed a faster activation of calcium-dependent chloride currents by intracellular application of IP3. A faster chloride current induction was observed in RPE cells from RCS rats compared to cells from nondystrophic rats, due to the increased calcium conductance in cells from RCS rats. The speed of chloride current induction in RPE cells from RCS rats could be reduced by the L-type channel blocker nifedipine. The increased calcium conductance in RPE cells from RCS rats is due to L-type calcium channels. Thus, L-type calcium channels change the response of RCS RPE cells to IP3 and may be part of the impaired regulation of phagocytosis observed in this rat strain.

The authors thank Dr. T. Weiser and Dr. F. Stumpff for helpful dis-

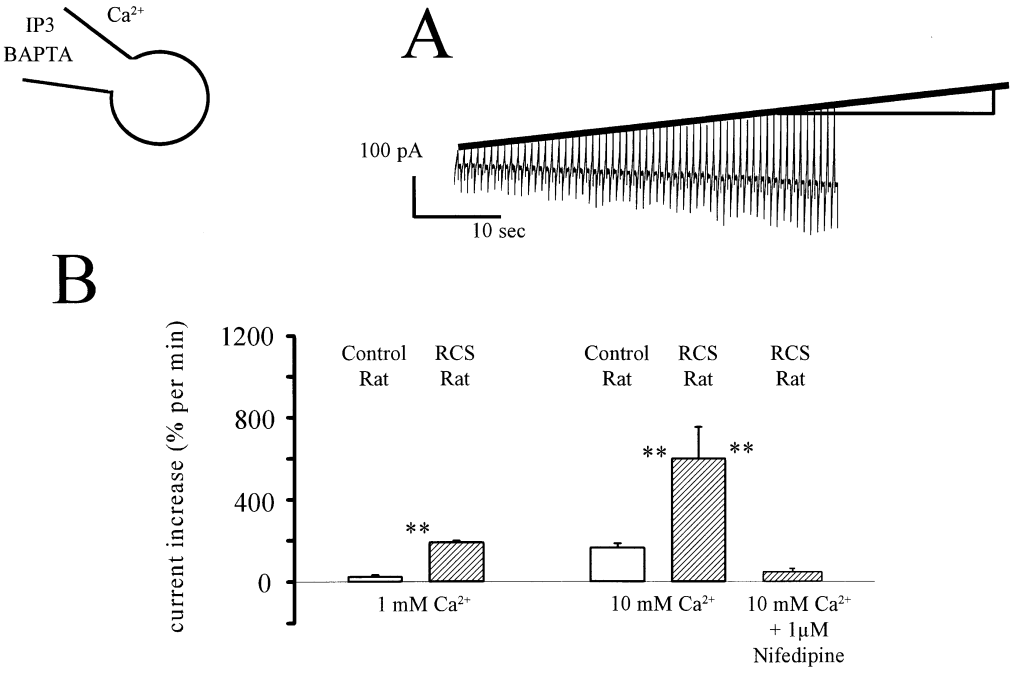

Fig. 8. Differences in Cl^--current activation by IP3 between cells from nondystrophic control rats and RCS rats. (*A*) To compare the activation of Cl^- currents by IP3 in RPE cells from RCS and nondystrophic rats the slope of Cl^--current activation was estimated. The slope of current activation was evaluated in the continuous recordings of the membrane conductance (HP = −45 mV) during the linear phase of outward current increase and calculated as increase of the current amplitude in one minute. This was expressed in percent of the current amplitude measured directly after breaking into the whole-cell configuration. (*B*) Comparison of the current increase induced by IP3 in RPE cells from RCS and nondystrophic rats. The currents were induced using BAPTA-pipette solution containing IP3 (10 μM) and bath solutions containing 10 mM or 1 mM Ca^{2+} (*see* the Table). In RPE cells from RCS rats, a significantly faster increase of current was observed with 1 mM and with 10 mM Ca^{2+} in the bath solution. The blocker for L-type calcium channels nifedipine (1 μM) could significantly reduce the increased current increase in RPE cells from RCS rats.

cussions, H. Morhardt for expert technical assistance. This work was supported by the Deutsche Forschungsgemeinschaft (grant Wi-992/1-3) and the Deutsche Retinitis Pigmentosa Vereinigung.

References

Bialek, S., Miller, S.S. 1994. K^+ and Cl^- transport mechanisms in bovine pigment epithelium that can modulate subretinal space volume and composition. *J. Physiol.* **475:**401–417

Botchkin, L.M., Matthews, G. 1993. Chloride current activated by swelling in retinal pigment epithelium cells. *Am. J. Physiol.* **265:**C1037–C1045

Botchkin, L.M., Matthews, G. 1994. Voltage-dependent sodium channels develop in rat retinal pigment epithelium cells in culture. *Proc. Natl. Acad. Sci. USA* **91:**4564–4568

Calahan, M.D., Lewis, R.S. 1988. Role of potassium and chloride channels in volume regulation by T-lymphocytes. *In:* Cell Physiology of the Blood. R.B. Gunn and J.C. Parker, editors. pp. 281–301. Rockefeller University Press, New York

Chaitin, M.H., Hall, M.O. 1983. Defective ingestion of rod outer segments by cultured dystrophic rat pigment epithelial cells. *Invest. Ophthalmol. Vis. Sci.* **24:**812–820

Edwards, R.B. 1977. Culture of rat retinal pigment epithelium. *In Vitro* **13:**301–304

Friedman, Z., Delahunty, T.M., Linden, J., Campochiaro, P.A. 1991. Human retinal pigment epithelial cells possess V_1 vasopressin receptors. *Curr. Eye Res.* **10:**811–816

Fujii, S., Gallemore, R.P., Hughes, B.A., Steinberg, R.H. 1992. Direct evidence for a basolateral membrane Cl^- conductance in toad retinal pigment epithelium. *Am. J. Physiol.* **262:**C374–C383

Gallemore, R.P., Steinberg, R.H. 1989*a*. Effects of DIDS on the chick retinal pigment epithelium. 1. Membrane potentials, apparent resistances and mechanisms. *J. Neurosci.* **9:**1968–1976

Gallemore, R.P., Steinberg, R.H. 1989*b*. Effects of DIDS on the chick retinal pigment epithelium: 2. Mechanism of the light peak and other responses originating on the basal membrane. *J. Neurosci.* **9:**1977–1984

Gallemore, R.P., Steinberg, R.H. 1990. Effects of dopamine on the chick retinal pigment epithelium. *Invest. Ophthalmol. Vis. Sci.* **31:**67–80

Gallemore, R.P., Steinberg, R.H. 1993. Light-evoked modulation basolateral membrane Cl^--conductance in chick retinal pigment epithelium: the light peak and fast oscillation. *J. Neurophysiol.* **70:**1669–1680

Gregory, C.Y., Abrams, T.A., Hall, M.O. 1992. cAMP production via the adenelyl cyclase pathway is reduced in RCS rat RPE. *Invest. Ophthalmol. Vis. Sci.* **33:**3121–3124

Griff, E.R. 1991. Potassium-evoked responses from the retinal pigment epithelium of the toad *Bufo marinus. Exp. Eye Res.* **53:**219–228

Hall, M.O., Abrams, T.A. 1991. RPE cells from normal rats do not secrete a factor which enhances the phagocytosis of ROS by dystrophic rat RPE cells. *Exp. Eye Res.* **52:**461–464

Hall, M.O., Abrams, T.A., Mittag, T.W. 1991. ROS ingestion by RPE cells is turned off by increased protein kinase C activity and by increased calcium. *Exp. Eye Res.* **52:**591–598

Halm, D.R., Frizzell, R.A. 1992. Anion permeability in an apical membrane chloride channel of a secretory epithelial cells. *J. Gen. Physiol.* **95:**97–120

Hamill, O.P., Marty, A., Neher, E., Sakmann, B., Sigworth, F.J. 1981. Improved patch-clamp techniques for high-resolution current recordings from cells and cell-free patches. *Pfluegers Arch.* **391:**85–100

Heth, C.A., Marescalchi, P.A. 1994. Inositol triphosphate generation in cultured rat retinal pigment epithelium. *Invest. Ophthalmol. Vis. Sci.* **35:**409–416

Heth, C.A., Schmidt, S.Y. 1992. Protein phosphorylation in retinal pigment epithelium of Long-Evans and Royal College of Surgeon rats. *Invest. Ophthalmol. Vis. Sci.* **33:**2839–2847

Hoth, M., Penner, R. 1993. Calcium-release-activated calcium current in rat mast cells. *J. Physiol.* **456:**359–386

Hughes, B.A., Segawa, Y. 1993. c-AMP activated chloride currents in amphibian retinal pigment epithelial cells. *J. Physiol.* **466:**749–766

Hughes, B.A., Steinberg, R.H. 1990. Voltage-dependent currents in isolated cells of the frog retinal pigment epithelium. *J. Physiol.* **428:**273–297

Joseph, D., Miller, S.S. 1991. Apical and basal membrane transport mechanisms in bovine retinal pigment epithelium. *J. Physiol.* **435:**439–463

Kirischuk, S., Scherer, J., Kettenmann, H., Verkhratsky, A. 1995. Activation of P_2-purinreceptors triggered by calcium release from InsP3-sensitive internal stores in mammalian oligodendrocytes. *J. Physiol.* **483.1:**41–57

Kennedy, B.G. 1994. Volume regulation in cultured cells derived from human retinal pigment epithelium. *Am. J. Physiol.* **266:**C676–C683

Kuno, M., Gardner, P. 1987. Ion channels activated by inositol 1,4,5-triphosphate in plasma membrane of human T-lymphocytes. *Nature* **326:**301–304

Kuno, M., Maeda, N., Mikoshiba, K. 1994. IP3-activated calcium-permeable channels in the inside-out patches of cultured cerebellar purkinje cells. *Biochem. Biophys. Res. Commun.* **199:**1128–1135

Kuriyama, S., Yoshimura, N., Ohuchi, T., Tanihara, H., Ito, S., Honda, Y. 1992. Neuropeptide-induced cytosolic Ca^{2+} transients and phosphatidylinositol turnover in cultured human retinal pigment epithelial cells. *Brain Res.* **579:**227–233

LaCour, M. 1992. Cl^- transport in frog retinal pigment epithelium. *Exp. Eye Res.* **54:**921–931

Liu, N.-P., Fitzgibbon, F., Nash, M., Osborne, N.N. 1992. Epidermal growth factor potentiates the transmitter-induced stimulation of c-AMP and inositol phosphates in human pigment epithelial cells in culture. *Exp. Eye Res.* **55:**489–497.

Marty, A., Tan, Y.P. 1989. The initiation of calcium release following muscarinic stimulation in rat lacrimal glands. *J. Physiol.* **419:**665–687

Matthews, G., Neher, E., Penner, R. 1989. Chloride conductance activated by external agonists and internal messengers in rat peritoneal mast cells. *J. Physiol.* **418:**131–144

McDonald, T.F., Pelzer, S., Trautwein, W., Pelzer, D.J. 1994. Regulation and Modulation of calcium channels in cardiac, skeletal, and smooth muscle cells. *Physiological Rev.* **74:**365–507

McLaren, M.J., Holderby, M., Brown, M.E., Inana, G. 1992. Kinetics of ROS binding and ingestion by cultured RCS rat RPE cells: modulation by conditioned media bFGF. *Invest. Ophthalmol. Vis. Sci.* **33:**1027A (*Abstr.*)

Neher, E. 1988. Calcium and secretion in dialysed mast cells. *J. Physiol.* **395:**193–214

Neher, E. 1992. Correction for liquid junction potentials in patch-clamp experiments. *In:* Methods in Enzymology Volume 207. B. Rudy and L.E. Iverson, editors. pp. 123–131. Academic Press, San Diego.

Osborne, N.N., Fitzgibbon, F., Nash, M., Liu, N.-P., Leslie, R., Cholewinski, A. 1993. Serotonergic, 5-HT_2, receptor-mediated phosphoinositide turnover and mobilization of calcium in cultured rat retinal pigment epithelium cells. *Vision Res.* **33:**2171–2179

Puck, T.T., Cieciura, S.J., Robinson, A. 1958. Genetics of somalian cells. 3. Long-term cultivation of euploid cells from human and animal subjects. *J. Exp. Med.* **108:**945–956

Rodriguez de Turco, E.B., Gordon, W.C., Bazan, N.G. 1992. Light stimulates in vivo inositol lipid turnover in frog retinal pigment epithelial cells at the onset of shedding and phagocytosis of photoreceptor membranes. *Exp. Eye Res.* **55:**719–725

Steinberg, R.H. 1985. Interactions between the retinal pigment epithelium and the neural retina. *Doc. Ophthalmol.* **60:**327–346

Strauss, O., Richard, G. and Wienrich, M. 1993. Voltage-dependent potassium currents in cultured human retinal pigment epithelial cells. *Biochem. Biophys. Res. Commun.* **191:**775–781

Strauss, O., Wienrich, M. 1993. Cultured retinal pigment epithelial cells from RCS rats express an increased calcium conductance in cultured rat retinal pigment epithelial cells. *J. Cell. Physiol.* **160:**89–96

Tao, Q., Rafuse, P.E., Kelly, M.E.M. 1994. Potassium currents in cultured rabbit retinal pigment epithelial cells. *J. Membrane Biol.* **141:**123–138

Ueda, Y., Steinberg, R.H. 1993. Voltage-operated calcium channels in fresh and cultured rat retinal pigment epithelial cells. *Invest. Ophthalmol. Vis. Sci.* **34:**3408–3418

Ueda, Y., Steinberg, R.H. 1994. Chloride currents in freshly isolated rat retinal pigment epithelial cells. *Exp. Eye Res.* **58:**331–342

Valverde, M.A., Diaz, M., Sepulveda, F.V., Gill, D.R., Hyde, C., Higgins, C.F. 1992. Volume-regulated chloride channels associated with the human multidrug-resistance P-glycoprotein. *Nature* **355:**830–833

Wen, R., Liu, G.M., Steinberg, R.H. 1993. Whole-cell recordings in fresh and cultured cells of the human and the monkey retinal pigment epithelium. *J. Physiol.* **465:**121–147

Wen, R., Liu, G.M., Steinberg, R.H. 1994. Expression of a tetrodotoxin-sensitive Na^+-current in cultured human retinal pigment epithelial cells. *J. Physiol.* **476:**187–196